Universal Passive Synchronization Method for Grid-Forming Inverters Without Mode Transition

Preprint

Heather Chang,[1] Nathan Baeckeland,[1]
Abhishek Banerjee,[2] and Gab-Su Seo[1]

1 National Renewable Energy Laboratory
2 Siemens

Presented at the IEEE ECCE Asia-International Conference on Power Electronics
Jeju, Korea
May 22–25, 2023

NREL is a national laboratory of the U.S. Department of Energy
Office of Energy Efficiency & Renewable Energy
Operated by the Alliance for Sustainable Energy, LLC

This report is available at no cost from the National Renewable Energy Laboratory (NREL) at www.nrel.gov/publications.

Contract No. DE-AC36-08GO28308

Conference Paper
NREL/CP-5D00-86972
August 2023

Universal Passive Synchronization Method for Grid-Forming Inverters Without Mode Transition

Preprint

Heather Chang,[1] Nathan Baeckeland,[1]
Abhishek Banerjee,[2] and Gab-Su Seo[1]

1 National Renewable Energy Laboratory
2 Siemens

Suggested Citation
Chang, Heather, Nathan Baeckeland, Abhishek Banerjee, and Gab-Su Seo. 2023. *Universal Passive Synchronization Method for Grid-Forming Inverters Without Mode Transition: Preprint*. Golden, CO: National Renewable Energy Laboratory. NREL/CP-5D00-86972. https://www.nrel.gov/docs/fy23osti/86972.pdf.

NREL is a national laboratory of the U.S. Department of Energy
Office of Energy Efficiency & Renewable Energy
Operated by the Alliance for Sustainable Energy, LLC

This report is available at no cost from the National Renewable Energy Laboratory (NREL) at www.nrel.gov/publications.

Contract No. DE-AC36-08GO28308

Conference Paper
NREL/CP-5D00-86972
August 2023

National Renewable Energy Laboratory
15013 Denver West Parkway
Golden, CO 80401
303-275-3000 • www.nrel.gov

NOTICE

This work was authored by the National Renewable Energy Laboratory, operated by Alliance for Sustainable Energy, LLC, for the U.S. Department of Energy (DOE) under Contract No. DE-AC36-08GO28308. Funding provided by U.S. Department of Energy Office of Energy Efficiency and Renewable Energy Solar Energy Technologies Office award numbers 38637 and 37770. The views expressed herein do not necessarily represent the views of the DOE or the U.S. Government. The U.S. Government retains and the publisher, by accepting the article for publication, acknowledges that the U.S. Government retains a nonexclusive, paid-up, irrevocable, worldwide license to publish or reproduce the published form of this work, or allow others to do so, for U.S. Government purposes.

Universal Passive Synchronization Method for Grid-Forming Inverters Without Mode Transition

Heather Chang*, Nathan Baeckeland*, Abhishek Banerjee‡, and Gab-Su Seo*†
*Power Systems Engineering Center, National Renewable Energy Laboratory, Golden, CO 80401, USA
‡Autonomous Systems and Control, Siemens, Princeton, NJ 08540, USA
e-mails: {heather.chang, nathan.baeckeland, gabsu.seo†}@nrel.gov, and abhishek.banerjee@siemens.com

***Abstract*—Power systems are transforming with increasing levels of inverter-based resources (IBRs). This transformation requires critical roles of grid-forming (GFM) inverters replacing synchronous generators for bulk power system stabilization and ancillary services, also allowing flexible power system operation, such as microgrid that is operated by multiple GFM IBRs to achieve system resilience against contingencies. To realize the resilient power systems allowing flexible in-and-out operation of GFM IBRs potentially programmed with different primary controls, a synchronization method universally applicable, i.e., independent of control types, would be beneficial to ease the integration process, but it has not been actively studied. To fill the gap, this paper proposes a universal synchronization method that achieves a passive synchronization to enable a smooth transition in a grid with off-nominal system parameters, i.e., voltage and frequency. The logic proposed requires no modification on the primary control, thus applicable to any type of GFMs with a voltage reference input. To validate the concept, a simulation of an IEEE 13-bus benchmark system modified with 3 GFM inverters is presented. It simulates an inverter-driven black start scenario in which GFM inverters autonomously turn on and connect to the grid under heavy loading, using the synchronization logic. The case study demonstrates that GFM inverters can tune their voltage reference to smoothly synchronize without severe transients, and contribute to a seamless black start of the grid under unbalanced load conditions. Two GFM methods—Droop and dispatchable virtual oscillator control—are used for the demo to validate feasibility and interoperability of the passive synchronization.**

***Index Terms*—Inverter synchronization, grid-forming inverter, inverter-based resources, passive synchronization, black start.**

I. Introduction

Today's electric grid is shifting towards increased generation from solar, wind, batteries, and more. These sources, also known as inverter-based resources (IBR), are connected to the power system with power electronic inverters rather than traditional large synchronous generators. The majority of inverters in today's grid are grid-following (GFL); they employ a phase-locked loop (PLL) to latch onto a well-defined stiff grid voltage and act as a current source. Therefore, in general, they are not capable of regulating voltage or frequency. As a result, they cannot inject power into the grid if no reliable external voltage reference exists. Grid-forming inverters (GFM), on the other hand, act as a voltage source. Based on the loading conditions, GFM inverters maintain the grid frequency and voltage, achieving power sharing between sources [1], [2]. As such, GFM inverters will be paramount to creating a flexible and resilient grid as the proliferation of IBRs increases.

With the transition to relying on IBRs to restore and form a stable grid, the control strategy for synchronizing GFM inverters before they get connected to the grid, is a critical research question for a number of reasons. First, the synchronization timing—the moment at which the GFM's circuit breaker is closed and the GFM is connected to the grid—will determine the short-time scale power flow between the inverter and the grid [3], [4]. This momentary power flow is inevitable, since it is faster than the inverter control dynamics, but it can be controlled based on the timing of closing the circuit breaker. Second, significant transients resulting from ineffective IBR synchronization may lead to system instability by forcing IBRs to experience extreme conditions that can saturate control loops and cause unexpected, destabilizing dynamic behavior [5], [6]. Third, the low short circuit ratio of IBRs, usually ranging in 1.1-1.5 p.u. compared to 6-10 p.u. of synchronous generators, translates into an increased risk of inverter tripping or early failure degrading reliability from repeated excursion to the out-of-range operations [7].

There are currently several synchronization methods found in literature. Introduced in [8], the synchronization method would work for all different types of GFM and GFL controls since the relay operation only uses local measurements and does not manipulate any signal in the IBRs. The architecture may not work, however, in a grid with off-nominal voltages as the voltage error does not reach an acceptable level (discussed more in Section II-B). Lu, in [9], proposed a synchronization method fully integrated in a virtual oscillator control (VOC) GFM. This method creates minimal transients as it allows the VOC to fully track the grid voltage before grid connection, but since the synchronization is embedded into the oscillator operation, it is not straightforward to extend it to other

This work was authored by the National Renewable Energy Laboratory, operated by Alliance for Sustainable Energy, LLC, for the U.S. Department of Energy (DOE) under Contract No. DE-AC36-08GO28308. This material is based upon work supported by the U.S. Department of Energy's Office of Energy Efficiency and Renewable Energy (EERE) under the Solar Energy Technologies Office Award Number 38637 and 37770.

GFM methods. Reference [10] presents a passive method that works for different GFM and GFL controls through monitoring signals with a PLL, similar to the industry practice [11]. However, it limits the conditions for synchronization so that if the frequency or voltage magnitude difference exceeds a programmed thresholds, synchronization will not occur. The traditional methods in [12], [13] may be used for GFM synchronization, potentially allowing for operation under off-nominal conditions. They involve a mode transition; an IBR operates in a GFL mode for synchronization and transitions to a GFM mode right after grid connection. In summary, there lacks a universal method that works regardless of GFM control approaches to allow a smooth transition for grid connection under off-nominal conditions without mode transition.

Considering the need for a more generally applicable methodology, this paper proposes a GFM synchronization method that minimizes synchronization transients and takes into account the off-nominal system conditions that may exist in IBR-heavy grids (e.g., a microgrid using higher droop gains to promote multiple-source power sharing that leads to more voltage and frequency deviations from nominal values). The proposed method adds a simple function block. This additional term is then combined with the voltage magnitude reference of a GFM primary control block to compose the synchronizing voltage. The term is only effective for pre-synchronization by nature, which means there is no need for a mode transition. As such, this novel approach allows for a smooth grid connection of GFM inverters without a mode transition or additional control coordination needed to ensure stability. Since it offsets the voltage reference only prior to synchronization, the method is applicable to any GFM controls with a voltage reference input. To realize the method, a passive synchronization logic is combined with this voltage reference tuning to monitor the error signal. It turns on the grid connection relay at a minimum error that suppresses short-circuit currents and leads to a power flow from the less loaded side with higher frequency (e.g., no-loaded inverters) to the more loaded side with lower frequency (e.g., the grid). This combination could also potentially facilitate a shorter settling time. This paper validates the passive synchronization method with the voltage tuning on the unbalanced IEEE benchmark system, 13-bus system. It demonstrates interoperation of GFM methods including droop and dVOC GFMs to validate the concept. The contributions of this paper are as follows:

- The proposed synchronization method allows for reliable grid connection of GFM IBRs and grid reconfiguration to deal with off-nominal voltage and frequency.
- It is applicable to any GFM method with a voltage reference, and no mode transition is required.
- The method requires no modification, and therefore, it has no dynamic effect on the existing controllers. The effect of the new term naturally disappears after grid connection.
- This paper provides validation of the concept with a simulation of an unbalanced IEEE benchmark system demonstrating three IBRs with Droop and dVOC GFMs collectively black starting the system under non-ideal grid and load conditions.

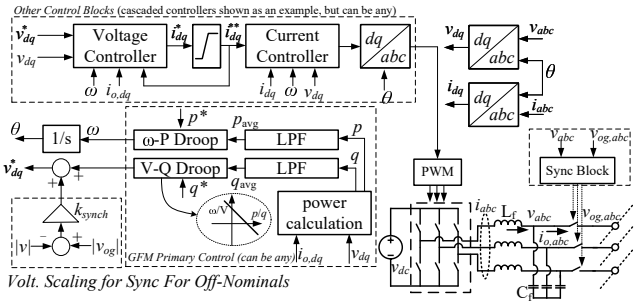

Fig. 1: Control diagram of a grid-forming inverter with the proposed synchronization method.

The paper is organized as follows. Section II discusses the synchronization method in detail and provides design criteria for the passive synchronization logic. Simulation results are shown in Section III for validation. Section IV concludes the paper.

II. Universal Synchronization for GFM Inverters Under Off-Nominal Conditions

This section introduces the concept of the new synchronization method and provides design considerations of the synchronization logic for its use in practice considering non-ideal grid conditions.

A. Synchronization for Non-ideal Operation Conditions

Fig. 1 illustrates the concept of the universal synchronization method proposed in this study. As shown, it scales the inverter-side voltage to be matched with the grid by feeding the difference between the voltages at the grid, $|v_{og}|$, and the inverter, $|v_o|$. It assumes that the GFM inverter is operational before grid connection to realize proper synchronization and to react to grid conditions. With the inverter-voltage magnitude scaled close to the grid voltage, the synchronization block monitoring the error signal from the two instantaneous voltages (discussed in detail later) closes the relays to connect the inverter to the grid. As implied by Fig. 1, the synchronization block operates in a passive manner as it does not modulate inner control variables. Since these two blocks do not affect the converter dynamics or require modification in the primary or other controls they can be straightforwardly implemented in any GFM type of controls with a voltage reference input. Notably, it is straightforward to integrate the method in GFM controls with additional controllers, such as virtual impedance control, as it does not modulate the system dynamics after grid connection.

The scaling input, $|v_{og}| - |v_o|$, is used to match the inverter voltage magnitude to the grid voltage to smoothen the relay closing transition. This is to overcome non-ideal grid conditions where the grid voltage is off nominal, e.g., when the grid is heavily loaded yielding undervoltage (such as in a black start using GFM inverters [14]) or when the GFM inverter for synchronization is located far way

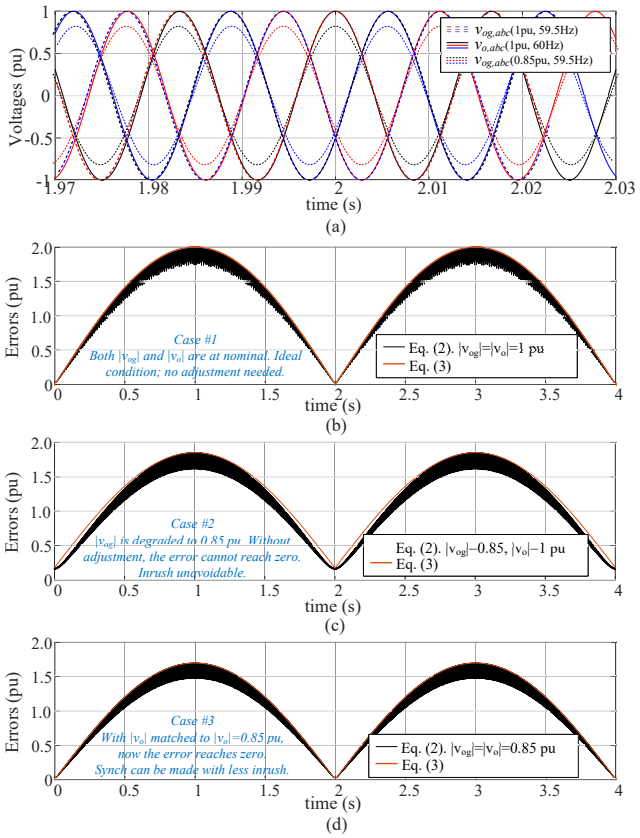

Fig. 2: Inverter and grid voltage and voltage error signals with and without voltage reference tuning when the grid voltage is degraded to 0.85 p.u. The grid is assumed at 59.5 Hz and the inverter at 60 Hz in this example: (a) three-phase voltage signals in different conditions around the zero error, (b) voltage error signal, κ_v with nominal voltages, i.e., $|v_{og}| = |v_o| = 1\ p.u.$ (c) error signal with degraded grid voltage without the proposed sync method, and (d) with the sync method.

from the other generators yielding a significant voltage deviation. With the method, GFM inverters can smoothly join the grid and contribute to improving the power quality. Control mode transition after grid connection is not required as the scaling input becomes zero once the inverter is connected to the grid, i.e., same potential. In case the two voltage signals (across the relay switch) are not available in the hardware, K_{synch} can be set to zero upon grid connection. In case the grid connection switches do not exist, i.e., inverter filters are always connected to the grid, the inverter modulation index signal can be used as a software switch, controlled by the method for the inverter start-up sequence [15].

B. Operation Principle of the Synchronization Method

This section discusses the operation of the synchronization method in detail with mathematical derivations. First, the two voltages (a-phase only shown), v_{og} and v_o can be expressed as:

$$\begin{aligned} v_{og,a} &= |V_{og}|cos(2\pi f_g t) \\ v_{o,a} &= |V_o|cos(2\pi f_{inv} t + \theta_0) \end{aligned} \tag{1}$$

where f_g and f_{inv} are the frequency of the grid and inverter, respectively. Since the relay short-circuits the two voltages, the transient currents are functions of the instantaneous voltage differences in each phase. To avoid detrimental inrush currents, the relays should close when the voltage differences are acceptable.

To identify the relay closing timing when the voltage differences are small, one can define a variable, voltage-difference factor, κ_v, to capture the three-phase voltage differences as (more details are found in [10], [16]):

$$\kappa_v = 0.5\left(|v_{og,a} - v_{o,a}| + |v_{inv,b} - v_{o,b}| + |v_{og,c} - v_{o,c}|\right). \tag{2}$$

Fig. 2 displays three examples with different grid and inverter voltage conditions that clarify the need for a synchronization method. The cases are: 1) when $|v_{og}| = |v_o| = 1$ p.u., 2) when $|v_{og}| = 0.85$ and $|v_o| = 1$ p.u., and 3) $|v_{og}| = |v_o| = 0.85$ p.u., illustrated in Fig. 2(b)-(d), respectively. The grid and inverter frequencies are fixed at 59.5 Hz and 60 Hz, respectively. To obtain insights and derive design equations, the envelop of the error signal can be approximated as:

$$\kappa_v < (|V_{og}|+|V_o|-2||V_{og}|-|V_o||)|sin(\pi\Delta f t)|+|V_{og}|-|V_o|. \tag{3}$$

Note that the voltage error signals for the three cases, as indicated in (3) and displayed in Fig. 2(b)-(d), are periodic with the frequency of $\Delta f = |f_g - f_{inv}|$ with different magnitude and offsets. Also notable is that the error signal reaches zero only when the grid and inverter voltage magnitudes are equal, i.e., $|V_{og}| = |V_o|$, yielding (3) to:

$$\kappa_v < (|V_{og}| + |V_o|)|sin(\pi\Delta f t)| \tag{4}$$

which justifies the voltage reference scaling in this study. In other words, if the voltages are not matched, inrush currents are inevitable. This confirms the benefit of tuning the voltage magnitude at the inverter matched to the grid to minimize the inrush current in the synchronization process.

Now, implementation of the method in different GFM controls is discussed. As mentioned, the method can be readily applied to any type of GFMs. In this study, three representative GFM methods are discussed: droop [17], [18], virtual synchronous machine [19], and dispatchable virtual oscillator control [15]. In case of droop, the voltage scaling can be integrated in the voltage droop, as illustrated in Fig. 1:

$$v^*_{d,droop} = v_{nom} + k_q(q^* - q) + \kappa_{synch}(|v_o| - |v_{og}|) \tag{5}$$

where $v^*_{d,droop}$ and v_{nom} are the resultant inverter voltage magnitude in steady state and the nominal voltage, and k_q is the voltage droop gain. As briefly discussed earlier, the adjustment term, $\kappa_{synch}(|v_o| - |v_{og}|)$, naturally becomes zero once the inverter is connected to a grid or κ_{synch} can be set zero if needed to avoid dynamic impact.

Similar to droop GFM, in dVOC GFM, the oscillator voltage reference v^* can be replaced by $v^* = v^* + \kappa_{synch}(|v_o| - |v_{og}|)$ that, in steady state, leads to:

$$\begin{aligned} v^*_{d,dvoc} \approx & v^\star_i + \frac{1}{\alpha(v^\star_i + \kappa_{synch}(|v_o| - |v_{og}|))}(q^\star - q) \\ & + \kappa_{synch}(|v_o| - |v_{og}|). \end{aligned} \tag{6}$$

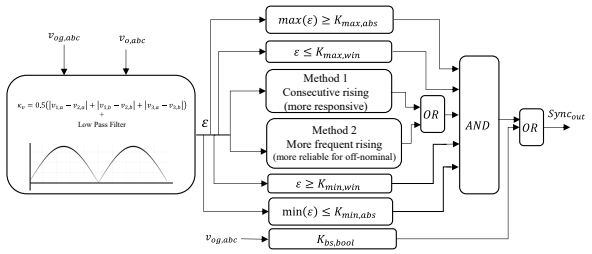

Fig. 3: Universal synchronization logic overview where ϵ is a low pass filtered error signal used for the logic. $K_{bs,bool}$ from $v_{og,abc}$ is used for the GFM that initiates the black start at zero grid voltage.

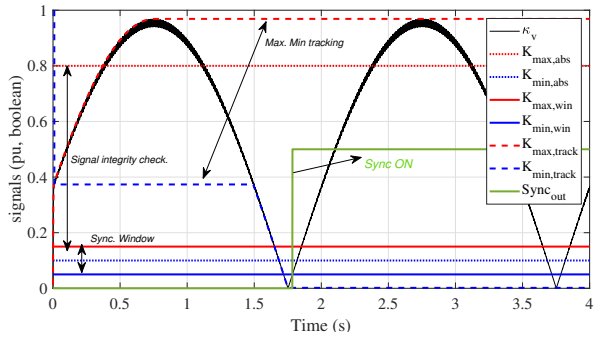

Fig. 4: Illustration of the synchronization logic operating under a grid voltage degraded at 0.5 p.u. with supplementary signals overlaid.

where $v^*_{d,dvoc}$ denotes the resultant inverter voltage magnitude and α is an oscillator coefficient to tune the reactive power droop and other dynamics [15]. As shown, it affects the effective reactive power droop gain as the voltage departs from the nominal, which underscores the importance of making sure the adjustment term disappears once the inverter is connected to the grid (which is naturally done by the proposed method).

For implementation in virtual synchronous machine GFM inverters, one can find the steady-state voltage equation:

$$v^*_{d,vsm} = v_{nom} + \frac{1}{D_q}(q^* - q) + \kappa_{synch}(|v_o| - |v_{og}|) \quad (7)$$

where $v^*_{d,vsm}$ is the scaled voltage magnitude and D_q is the equivalent voltage droop term.

C. Design Considerations for Universal Synchronization

To synchronize a GFM inverter to a preformed grid, the condition of the error signal is analysed as shown in Fig. 3. The parameters in Fig. 3 are each analyzed later in detail. Once the conditions are met, *AND* gated, the inverter relay will close. An example with an error signal and supplementary variables used is illustrated in Fig. 4. In this example, the grid has a frequency of 59.5 Hz while the inverter is operating at 60 Hz. The voltage magnitude of both the grid and inverter is set to 0.5 p.u., assuming the GFM voltage scaling is in place. The error signal shows two complete periods for illustration, but note that the error becomes zero once the relay closes. To avoid a significant inrush current, the voltage difference should be less than a certain value; the error signal should be close to zero at the switch closing.

In addition, note that the switch closing may facilitate the momentary power flow in a desired direction. For instance, the GFM inverter joining the grid—if supposed to share the system load with other GFMs—can be driven by controlling the switch closing timing to inject power into the grid during the transient. It may facilitate the system to settle smoothly to the new steady state. This can be realized by closing the relay when the error signal increases. As shown in Fig. 2, this ensures the voltages in the less loaded side (thus at higher frequency, i.e., inverter side in this example) are slightly leading the voltages in the other side, more loaded, (thus at lower frequency, i.e., grid side in this example). This forces the momentary power flow from the less loaded side to the more loaded side, same direction for the new steady state. More discussion can be found in [8]. In practice, one should account for the turn-on delay of the relay that may incur non-ideal transients, but that can likely be compensated for. Moreover, the momentary power exchange control with the relay close timing may not be guaranteed as the electrical distance between sources increases, as shown in Section III, which can be a future direction.

1) Key variables:

- Cutoff frequency of the low-pass filter to process the error signal. A low-pass filter is necessary to filter out $6th$ harmonic of the grid frequency in the error signal, i.e., 360 Hz in a 60 Hz grid, and other erroneous measurements from noise and computation. On the other hand, it must allow all signals of $2\pi\Delta f_{max}$ to pass through with acceptable attenuation and delay or a significant delay will occur. These two conditions indicate that: $2\pi\Delta f_{max} < f_{LPF} < 6\omega_{nom}$. Δf_{max} can be determined by frequency droop gains of GFM inverters. Based on these two considerations, the cutoff frequency of the low-pass filter is designed at 100 Hz, to avoid signal attenuation at Δf_{max}=1.2 Hz, i.e., to accommodate 2% droop, in the simulation shown in Section III. With this design choice, the 360 Hz ripple still impacts the signal, which necessitates additional signal processing as discussed hereafter.
- Counter value $K_{num,rises}$, to capture the rising edge. As mentioned, the relay should close shortly after the error signal passes the minimum and starts increasing [8], [16]. This parameter sets the number of calculated rises necessary for the relay switch to be turned on. A greater counter number makes the switching more reliable, but it may cause a delay, especially under noisy measurements. If the number is too large, then the enable signal will only turn on when the error becomes too large and the circuit breaker will not close as other conditions are not satisfied. Therefore, the design should consider the worst case that occurs when $\Delta f = \Delta f_{max}$ and the $V_1 = V_2 = V_{nom}$ in which the error signal will rise at the steepest slope. With a given sampling time of the measurement, T_s, the minimum number of samples (the worst case), N_{min}, can be calculated between

TABLE I: System Setup and GFM Inverter Parameters for Simulation.

Item	Design Selections
Baseline Load (MW, MVar)	P_a = 1.16, P_b = 0.97, P_c = 1.14 Q_a = 0.61, Q_b = 0.63, Q_c = 0.75
Transient at 5 s	3.6 MW at bus 671
Inverter Parameters	P_{rated} = 3.6 MVA, V_{rated} = 1000 V, L_{f} = 0.04, R_{f} = 0.054, C_{f} = 0.1 L_{g} = 0.06, R_{g} = 0.005
Droop GFM	k_p = 0.03, k_q = 0.15, ω_{n} = $2\pi \cdot 60$ rad/sec
dVOC GFM	α = 14.4, η = 2.094

*Quantities are in per unit if not specified.

TABLE II: Sync Logic Parameters Used in Simulation with $T_s = 125\ \mu s$.

Item	Design Selections
$K_{num,rises}$	38
$K_{bs,bool}$	16000
$K_{max,abs}$	1.6
$K_{min,abs}$	0.05
$K_{max,win}$	0.01
$K_{min,win}$	0.12

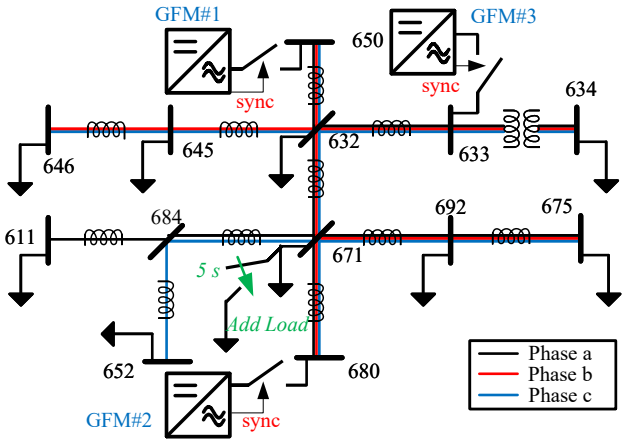

Fig. 5: Modified IEEE 13-bus system with 3 GFM inverters: GFM #1&2 with droop and GFM #3 with dVOC GFM to test the proposed universal synchronization logic and interoperability.

the window of $K_{min,win}$ to $K_{max,win}$ which are discussed later:

$$K_{num,rises} << N_{min} = \frac{K_{max,win} - K_{min,win}}{2\pi \Delta f_{max} T_s}. \tag{8}$$

- $K_{bool,rise}$. This parameter checks if the error signal is rising. Because of the 360 Hz ripple, a simple comparison between consecutive samples cannot be used. Instead, two complementary methods are used to detect whether the error signal is rising. One ignores the ripple by counting consecutive rises and ignoring a small number of consecutive falls caused by the 360 Hz ripple. Once there are a certain number of consecutive falls, then the signal is reset. The benefits of this method are that it can be readily implemented and it requires less calculations, but its performance degrades in conditions when the frequency differences (and the voltage magnitude) are small, leading to the flattened slope of error signal, which necessitates a complementary method. The other method measures the numeric amount the signal rises and the amount it falls in each ripple. If it rose more than it fell for a given ripple, then the period is classified as rising. This method requires more calculations and it performs well at degraded voltages and small frequency differences. These two logics are *OR* gated and yields $K_{bool,rise}$, as illustrated in Fig. 3.
- $K_{bs,bool}$. This Boolean signal will override all other parameters to allow a black start. When no voltage exists in the grid side, a GFM inverter should establish the voltage on the grid. In case there are multiple black-start capable GFM inverter units, additional intelligence can be implemented to organize the restoration process, e.g., programming a turn-on delay inversely proportional to the inverter capability to eliminate or minimize the need for communication [10]. If it detects that the signal has been under a threshold for a preset amount of time, the GFM inverter will automatically turn on as illustrated in Fig.3.

2) Supplementary Variables:

- $K_{max,abs}$: This absolute error value is programmed considering the maximum voltage deviation of $|v_{og}|$ acceptable from the nominal voltage. $max(\epsilon) > K_{max,abs}$ yields a high signal. $max(\epsilon)$ is initialized at 0 p.u. and tracks the maximum of the error signal. This parameter ensures that the signal is reasonable and that at least half of a cycle has passed before the relay closes, i.e., to avoid a premature switching.
- $K_{min,abs}$: This absolute error value is programmed considering the maximum mismatch between $|v_{og}|$ and $|v_o|$ to be acceptable. $min(\epsilon) < K_{min,abs}$ yields a high signal. $min(\epsilon)$ is initialized at 2 p.u. and tracks the minimum of the error signal. Similar to $K_{max,abs}$, this parameter ensures that the signal is reasonable and that at least half of a cycle has passed before relay closing. It will also serve as a check to ensure that the magnitudes of the two voltage signals are close enough, which may be used for tuning.
- $K_{max,win}$ and $K_{min,win}$: These two preset variables form a switch close window as illustrated in Fig. 4. $K_{max,win}$ sets the maximum error value that allows the relay turn on; $\epsilon < K_{max,win}$ yields a high signal. This ensures that the inverter relay is not turned on too late which may yield a detrimental inrush current. $K_{min,win}$ sets the minimum error value for switch turn on; $\epsilon > K_{min,win}$ yields a high signal. This variable also serves a similar function as $K_{num,rises}$ but acts as a secondary security measure; it ensures that the breaker is not closed too early.

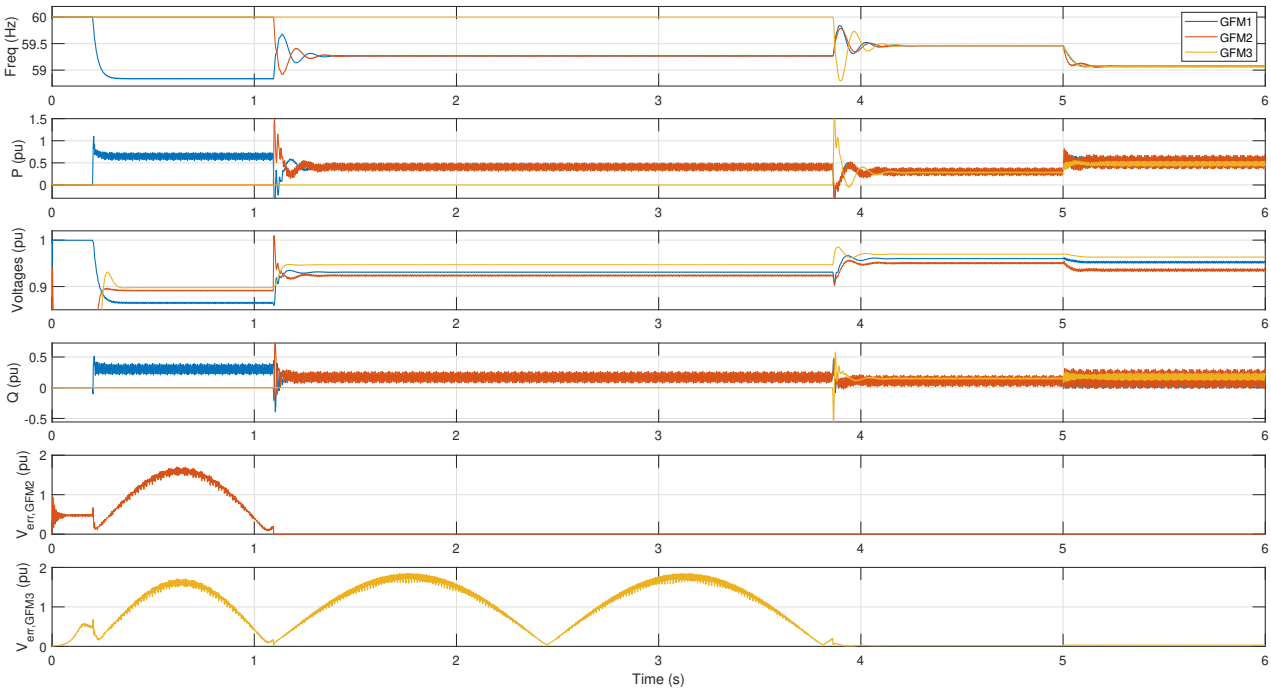

Fig. 6: Entire black-start simulation result with 3 GFM inverters and the proposed synchronization logic: from the top, frequencies of all 3 GFM inverters, active powers, rms voltages, reactive powers, filtered voltage error signal in GFM #2, and voltage error signal in GFM #3.

III. Simulation Results

To validate the universal GFM synchronization concept, this section presents simulation results. For the simulation, the IEEE 13-bus benchmark system has been modified to have three GFM inverters, GFM #1-3, connected to bus 650, 680, and 633, respectively. Fig. 5 illustrates the test system. To emulate a black start scenario in a microgrid setup, the voltage source at the substation has been removed and the three GFM inverters collectively black start the system from the zero voltage. System baseline loading is the same with the original model representing an unbalanced distribution system, as shown in Table I. Combination of the distributed GFM inverters and the unbalanced system loading will demonstrate the GFM control and system dynamic behavior under non-ideal conditions. After all three GFM inverters involved in the process of bringing the system parameters near nominal with the baseline load, an active power load transient occurs at bus 671 at t=5 s which emulates additional load pick up.

GFM inverters are equipped with the synchronization logic proposed with the parameters specified in Table II. Arbitrary start-up delays (to activate the logic) have been programmed to emulate an autonomous black start process based on the logic. To validate the universal application of the logic as discussed in Section II-B, GFM #1&2 employ droop and GFM #3 dVOC. Inverter parameters are tabulated in Table I. Inner control loops are not implemented for this evaluation. Notable are the voltage droop gains for GFM inverters. To evaluate the performance of the universal synchronization under degraded voltage conditions, a relatively high, 15% of voltage droop is adopted in this study, which would result in large voltage deviations from the nominal. GFM synchronization under off-nominal conditions is important because i) GFM inverters are the foundation to stabilize the high IBR penetration grid with reduced system inertia, so their robust synchronization is paramount, and ii) it would improve the resilience of the grid by unlocking potential use cases, including inverter-driven black start that may experience severe voltage degradation due to lacking capacity that requires additional GFM units to join to fully establish the grid.

Fig. 6 displays the simulation result. GFM #1, programmed with shortest activation delay, initiates the black start in the zero voltage grid. Due to the loading, the system voltage settles at an off-nominal value. Oscillations in active and reactive power are observed due to the unbalanced loading and positive-sequence-based control. Once the grid voltage established by GFM #1, the synchronization logic of GFM #2&3 start tracking the voltage error. Around t=1.1 s, GFM #2 turns on when the instantaneous voltage differences are acceptable while GFM #3 keeps tracking the signal since it is not activated yet. After connecting to the grid, the two GFM inverters redistribute the system loading, increasing the system voltage further. Activated afterwards, GFM #3, programmed with dVOC, also joins the grid around t=3.8 s, leading the system to a new steady state with increased voltage and frequency nearer to the nominal. It demonstrates the universal synchronization applicable to different GFMs and interoperability. At t=5 s, a 3.6 MW load is added to the system to emulate additional load pick up. All three GFM inverters collectively regulate the grid by sharing the

additional load. It completes the black start scenario.

IV. Conclusion and Future Work

This paper has presented a universal synchronization method that is applicable to any GFM inverter with a voltage reference input without affecting the control dynamics. Since the effect of the method naturally disappears once the GFM is grid connected, no mode transition is required. The concept has been validated by the simulation of the IEEE 13-bus system with three GFM inverters, each programmed with droop or dVOC. It demonstrates that GFM inverters can synchronize to the grid under off-nominal conditions by matching the inverter terminal voltage to the grid, which will facilitate the future research and development for inverter-driven black start with multiple GFM inverters for a large system baseline load and GFM inverter's fault behavior study and improvement. This study can also be extended i) to test more types of GFMs, including virtual synchronous machine and matching control, ii) to involve inner control loops and current limit functions to relate overloading and fault conditions, and iii) to conduct experimental verification for field deployment.

References

[1] J. Matevosyan, J. MacDowell, N. Miller, B. Badrzadeh, D. Ramasubramanian, A. Isaacs, R. Quint, E. Quitmann, R. Pfeiffer, H. Urdal, T. Prevost, V. Vittal, D. Woodford, S. H. Huang, and J. O'Sullivan, "A future with inverter-based resources: Finding strength from traditional weakness," *IEEE Power and Energy Magazine*, vol. 19, no. 6, pp. 18–28, 2021.

[2] D. B. Rathnayake, M. Akrami, C. Phurailatpam, S. P. Me, S. Hadavi, G. Jayasinghe, S. Zabihi, and B. Bahrani, "Grid forming inverter modeling, control, and applications," *IEEE Access*, vol. 9, pp. 114 781–114 807, 2021.

[3] A. Sajadi, R. W. Kenyon, and B.-M. Hodge, "Synchronization in electric power networks with inherent heterogeneity up to 100% inverter-based renewable generation," *Nature Communications*, vol. 13, no. 1, 5 2022.

[4] D. Sharma, F. Sadeque, and B. Mirafzal, "Synchronization of inverters in grid forming mode," *IEEE Access*, vol. 10, pp. 41 341–41 351, 2022.

[5] L. Huang, H. Xin, Z. Wang, L. Zhang, K. Wu, and J. Hu, "Transient stability analysis and control design of droop-controlled voltage source converters considering current limitation," *IEEE Transactions on Smart Grid*, vol. 10, no. 1, pp. 578–591, 2017.

[6] E. Rokrok, T. Qoria, A. Bruyere, B. Francois, and X. Guillaud, "Transient stability assessment and enhancement of grid-forming converters embedding current reference saturation as current limiting strategy," *IEEE Transactions on Power Systems*, vol. 37, no. 2, pp. 1519–1531, 2021.

[7] D. Kim, H. Cho, B. Park, and B. Lee, "Evaluating influence of inverter-based resources on system strength considering inverter interaction level," *Sustainability*, vol. 12, no. 8, 2020. [Online]. Available: https://www.mdpi.com/2071-1050/12/8/3469

[8] R. H. Lasseter, "Control and design of microgrid components," *PSERC Publication 06-03*, 2006.

[9] M. Lu, S. Dutta, V. Purba, S. Dhople, and B. Johnson, "A pre-synchronization strategy for grid-forming virtual oscillator controlled inverters," in *2020 IEEE Energy Conversion Congress and Exposition (ECCE)*, 2020, pp. 4308–4313.

[10] A. Banerjee, A. Pandey, U. R. Pailla, G.-S. Seo, S. Shekhar, H. Jain, Y. Lin, X. Wu, J. Bamberger, and U. Muenz, "Autonomous microgrid restoration using grid-forming inverters and smart circuit breakers," in *2022 IEEE Power & Energy Society General Meeting (PESGM)*, 2022, pp. 1–5.

[11] "Synchronization systems," (Date last accessed 16-March-2023). [Online]. Available: https://selinc.com/engineering-services/synchronization/

[12] J. Wang, A. Pratt, and M. Baggu, "Integrated synchronization control of grid-forming inverters for smooth microgrid transition," in *2019 IEEE Power & Energy Society General Meeting (PESGM)*, 2019, pp. 1–5.

[13] A. Yazdani and R. Iravani, *Voltage-sourced converters in power systems*. Wiley-Blackwell, 2010.

[14] J. Sawant, G.-S. Seo, and F. Ding, "Resilient inverter-driven black start with collective parallel grid-forming operation," in *Proc. IEEE Innovative Smart Grid Technologies Conference*, 2023, pp. 1–5.

[15] G.-S. Seo, M. Colombino, I. Subotic, B. Johnson, D. Groß, and F. Dörfler, "Dispatchable virtual oscillator control for decentralized inverter-dominated power systems: Analysis and experiments," in *Proc. 2019 IEEE Applied Power Electronics Conference and Exposition (APEC)*, 2019, pp. 561–566.

[16] A. Banerjee, V. Pawaskar, A. Pandey, G.-S. Seo, U. R. Pailla, X. Wu, and U. Muenz, "Autonomous restoration of networked microgrids using communication-free smart sensing and protection units," *IEEE Transactions on Sustainable Energy*, in press.

[17] A. Husna, M. A. Roslan, and M. H. Mat, "Droop control technique for equal power sharing in islanded microgrid," *International Journal of Power Electronics and Drive Systems (IJPEDS)*, vol. 10, p. 530, 03 2019.

[18] Y. Lin, J. H. Eto, B. B. Johnson, J. D. Flicker, R. H. Lasseter, H. N. Villegas Pico, G.-S. Seo, B. J. Pierre, and A. Ellis, "Research roadmap on grid-forming inverters," 11 2020. [Online]. Available: https://www.osti.gov/biblio/1721727

[19] H.-P. Beck and R. Hesse, "Virtual synchronous machine," in *2007 9th International Conference on Electrical Power Quality and Utilisation*, 2007, pp. 1–6.